REAL-TIME MONITORING OF BUILDING ENERGY BEHAVIOUR: A CONCEPTUAL FRAMEWORK

Alexandre Nassiopoulos[1], Frédéric Bourquin[2]
[1,2] Université Paris-Est, Laboratoire central des ponts et chaussées (LCPC), Paris, France.
[1] alexandre.nassiopoulos@lcpc.fr
[2] frederic.bourquin@lcpc.fr

ABSTRACT

This paper presents a conceptual framework for the continuous monitoring of buildings energy state. The proposed methodology is based on a reduced number of low-cost temperature and power sensors. It uses an inversion procedure to combine in an optimal way a detailed thermal model of the building envelope and the measurements obtained from temperature sensors. The inversion procedure aims at reconstructing the unknown right-hand side terms of a detailed thermal model thus enabling to quantify the various heat transfers between the building and its environment and between the different components of the building envelope.

INTRODUCTION

The improvement of building energy efficiency requires a better assessment of their global energy behavior over time. Monitoring systems can lead to significant reductions of the global energy use by increasing occupants' awareness of the consumptions or by enabling the implementation of more efficient regulation strategies (Burgess and Nye (2008)). In commercial buildings for instance, some studies suggest that up to 40% energy savings can be made by closer supervision and monitoring (O'Sullivan et al. (2004), Salsbury and Diamond (2005)). Various monitoring strategies have been under study in the recent years. For instance, the so-called continuous commissioning approach aims at resolving operating problems, improving comfort, optimizing energy use and identifying retrofits (Neumann and Jacob (2008)). Partly motivated by the environmental concern and consequent regulations, the building construction practices evolve towards a more performance-based building approach in which the concern becomes the performance of the final building rather than the means employed to construct it (Glaser and Tolman (2008)). All these applications rely somehow on the ability to accurately predict a system's behavior using a calibrated model (Liu (1999)). Collecting data on the real building during operation is essential to analyze energy performance in applications where the accurate efficiency prediction is critical, such as diagnostics in view of retrofitting, energy services or evaluation in the mark of performance-based contracts.

Simulation and numerical modeling offer a great support for such monitoring and diagnostic applications (Clarke et al. (2004)). However, they often fail to predict accurately the actual performance (Haves et al. (2001)) because of a bad knowledge of the actual occupation scenarios and environmental conditions (Richalet et al. (2001)). For instance, Branco et al. (2004) present a long term study on a high efficiency building and conclude that most of the differences between real and predicted consumptions were due to usage conditions. Krüger and Givoni (2008) showed that model-based consumption prediction can be up to 100% wrong if meteorological data is collected in a nearby meteorological station rather than on site.

In other terms, what is at issue is the big gap that exists between the accuracy of the modeling tools and the accuracy of the input data for these tools. To reduce this gap, the strategy can either be to reduce the level of detail of the model, or to resort to an extended instrumentation system.

In the first kind of approach, on-site measurements are used to identify the parameters of a reduced model of the building. The reduced model can either be obtained by simple or multiple parameter regression, or by a simplified modeling of the dynamic behavior using equivalent thermal parameters (see Santamouris (2005), MacDonald and Wasserman (1989) and references therein). This kind of approach constructs efficient tools to predict energy behavior or to evaluate and compare existing buildings (Subbarao et al. (1988),Madsen and Holst (1995)). However, it does not take advantage of the high accuracy on the component level that can be achieved with today's dynamic simulation codes, and is thus less suited for comparing design concepts or retrofit scenarios.

The second kind of approach relying on an important effort to instrument extensively the building leads to expensive and difficult-to-implement operations, and thus is not suited for an extensive use. As a matter of fact, a good monitoring system should be as less intrusive as possible, to avoid interactions with the occupants, should be based on robust sensor technology and should be low-cost in or-

der to meet cost efficiency requirements (Piette, Kinney, and Haves (2001), Glaser and Tolman (2008)). Moreover, it should enable to distinguish between the occupation and the environmental effects on the building consumptions.

The present work proposes a conceptual framework for the development of a building energy monitoring system offering both detailed modeling and reduced instrumentation cost. It consists in combining in an optimal way the measurements given by temperature and power sensors, both widely used in construction and not expensive, and a detailed heat transfer model based on usual dynamic multizone simulation assumptions. Using an inversion procedure, the measurements serve to reconstruct the unknown source terms of the detailed model. Once the source terms (the right-hand side of equations) are known, the model enables the quantitative assessment of the various energy transfers which occur between the environment and the building, as well as between the different components of the building envelope. This framework allows to keep the full benefit of using a detailed model where the parameters refer to real characteristics (physical properties of materials, wall widths, ...) of the building.

The inverse procedure relies upon optimal control theory (Lions (1968)). The temperature measurements are compared to the response of the heat transfer model. The minimization of a quadratic criterion measuring the discrepancy between sensor and model outputs yields the desired quantities. Tikhonov regularization is used in order to deal with the ill-posedness of the inverse problem (Engl, Hanke, and Neubauer (1994)). The minimization is done using the adjoint method (Alifanov (1994)) which constructs easy-to-implement algorithms. In a previous work, the authors presented a mathematical framework that enables the fast and accurate reconstruction of the different unknown quantities at present time (Bourquin and Nassiopoulos (2010)). The resulting reconstruction tools are well suited for real-time applications.

The methodology is presented here on a simple test case representing most of the transfer phenomena occurring within a one-zone building. However, on-going research work shows evidence that it could be extended to complex buildings.

PROBLEM FORMULATION

Test-case and modeling assumptions

The model on which is based the monitoring procedure uses the standard multizone assumptions (Clarke (2001)). It is presented here in a generic representation based on the heat transfer equations in each zone and in each wall in order to keep some generality.

The test-case under study consists of a single room with four walls and a window, as depicted on figure 1. If one makes the assumption that the comfort conditions within a given space zone are homogeneous, then this zone can be represented by a single node with a time-varying temperature. Here, the room is assumed to correspond to one zone. This zone is subject to a thermal loading following at least three flow-paths: direct convective heat from heating systems or other appliances (represented by the function Q), heat due to air flow (represented by the function R) from outside and/or adjacent zones, and convective exchanges with the surrounding walls.

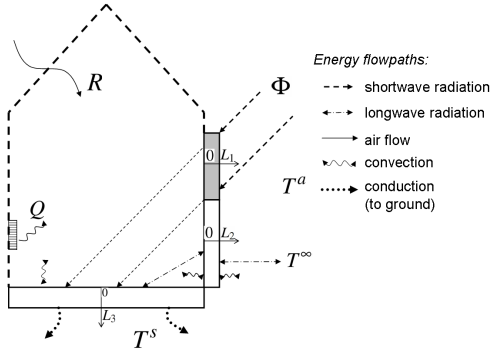

Figure 1: The simplified test-case.

Each wall exchanges energy by convection with the air inside the zone and with the external environment. It also exchanges energy by longwave radiation with other facing walls (inside) and with the external environment assumed to be at the equivalent temperature T^∞ (corresponding to the so-called sky temperature (Clarke (2001))). External wall surfaces are subject to solar shortwave radiation Φ. A portion α of this solar radiation is absorbed by transparent glazings and another portion $(1-\alpha)$ is incident on the inside ground walls. Heat transfer within each solid wall takes place by conduction. We only consider conduction transfer in one-dimension, thus making the assumption of homogeneous characteristics along the two other dimensions.

To further simplify the presentation of the method, two opaque walls (the outside vertical wall and the ground wall) and a transparent one (the glazing of the window) are modeled only (see figure 1). We denote T the temperature inside the zone and θ_i the temperatures within each wall i. The evolution of T and θ_i, $i = 1..3$ is given by the

following set of transient equations:

$$\begin{cases} \rho_1 c_1 \dfrac{\partial \theta_1}{\partial t} - \dfrac{\partial}{\partial x} k_1 \dfrac{\partial \theta_1}{\partial x} = 0 & [0,L_1]\times[0,\tau] \\ -k_1 \dfrac{\partial \theta_1(0,t)}{\partial x} + (2h_r + h_v)\theta_1(0,t) & \\ \quad -h_r(\theta_2(0,t)+\theta_3(0,t)) - h_v T = 0 & [0,\tau] \\ k_1 \dfrac{\partial \theta_1(L_1,t)}{\partial x} + (h_r+h_v)\theta_1(L_1,t) = & \\ \quad h_r T^{\infty} + h_v T^a + \Phi & [0,\tau] \\ \theta_1(x,0) = 0 & [0,L_1] \end{cases} \tag{1}$$

$$\begin{cases} \rho_2 c_2 \dfrac{\partial \theta_2}{\partial t} - \dfrac{\partial}{\partial x} k_2 \dfrac{\partial \theta_2}{\partial x} = 0 & [0,L_2]\times[0,\tau] \\ -k_2 \dfrac{\partial \theta_2(0,t)}{\partial x} + (2h_r + h_v)\theta_2(0,t) & \\ \quad -h_r(\theta_1(0,t)+\theta_3(0,t)) & \\ \quad -h_v T = (1-\alpha)\Phi & [0,\tau] \\ k_2 \dfrac{\partial \theta_2(L_2,t)}{\partial x} + h_s \theta_2(L_2,t) = h_s T^s & [0,\tau] \\ \theta_2(x,0) = 0 & [0,L_2] \end{cases} \tag{2}$$

$$\begin{cases} \rho_3 c_3 \dfrac{\partial \theta_3}{\partial t} - \dfrac{\partial}{\partial x} k_3 \dfrac{\partial \theta_3}{\partial x} = \alpha\Phi & [0,L_3]\times[0,\tau] \\ -k_3 \dfrac{\partial \theta_3(0,t)}{\partial x} + (2h_r + h_v)\theta_3(0,t) & \\ \quad -h_r(\theta_1(0,t)+\theta_2(0,t)) & \\ \quad -h_v T = 0 & [0,\tau] \\ k_3 \dfrac{\partial \theta_3(L_3,t)}{\partial x} + (h_v+h_r)\theta_3(L_3,t) = & \\ \quad h_v T^a + h_r T^{\infty} & [0,\tau] \\ \theta_3(x,0) = 0 & [0,L_3] \end{cases} \tag{3}$$

$$\begin{cases} C\dfrac{dT}{dt} + \displaystyle\sum_{i=1}^{3} h_v S_i (T - \theta_i(0,t)) + \rho_a c_a R T = & \\ \quad \rho_a c_a R T^a + Q & [0,\tau] \\ T(0) = 0 & \end{cases} \tag{4}$$

In the above equations, $t \in [0,\tau]$ is the time variable and x is the space variable in the domains $[0,L_i]$ corresponding to each wall i. We will use here the convention that the end point $x = L_i$ corresponds to the external face of the wall (see figure 1). For each wall i, ρ_i is the mass density, c_i the specific heat capacity and k_i the conductivity coefficient. These quantities may be space dependent. C is the total heat capacity of the zone and ρ_a, c_a the mass density and specific heat capacity of air.

Fourier-Robin representation is used for the boundary conditions. The convective heat exchange between an opaque or transparent wall i and the internal (respectively, external) air at temperature T (respectively, T^a) is given by the quantity $h_v(\theta_i - T)$ (respectively, $h_v(\theta_i - T^a)$). The heat exchange from the ground at temperature T_s to the external face of wall number 2 is given by $h_s(T^s - \theta_2)$.

Radiative heat exchanges are taken into account using equivalent exchange coefficients h_r. The underlying assumption is that the temperature differences stay small so that a linearization is valid. This makes possible to represent radiative exchange using Fourier-Robin boundary conditions like for the convective heat transfers. For instance, radiative heat exchange from wall i to wall i' will be denoted $h_r(\theta_i(0,t) - \theta_{i'}(0,t))$.

The equations (1) to (4) are coupled due to the convective and radiative terms. In the computational procedure they all have to be treated simultaneously.

These state-of-the-art modeling assumptions are used by most multizone simulation codes today (Clarke (2001)). The resolution of the heat transfer equations depends on the code. For instance, in TRNSYS (TRNSYS16 (2006)), from which the test data presented in the sequel were obtained, the equations are solved in an iterative way using equivalent transfer functions.

Problem formulation

In order to be able to characterize the energy state of the building at any time, one has to be able to solve the model equations (1) to (4). To do this, it is necessary to know the right-hand-side terms of these model equations. The monitoring problem thus consists in identifying the unknown sources and boundary conditions, *i.e.* the set of unknowns $\{Q, R, \Phi, T^{\infty}\}$. This can be achieved by making use of the measurements: the unknowns are sought so that the solutions of the set of equations (1)-(4) at sensor locations correspond to the measurements.

Consider 4 temperature sensors located at the external and internal surfaces of the vertical wall, at the internal surface of the ground wall, and one on the glazing of the window. They deliver transient measurements over time which will be denoted $\{\vartheta_\ell^d(t)\}_{\ell=1}^4$ in what follows. Note that only surface temperature sensors are used, so that the instrumentation be not intrusive (no need to drill the wall). The measurements are recorded during the time interval $[0,\tau]$, τ being the length of the observation period.

However, it proves impossible to recover both Q and R simultaneously using this instrumentation setup. This is due to the fact that both variables have the same effect on the observed temperatures. As a matter of fact, for a given external temperature T^a, substituting an impulse for R or Q will have the same effect on the zone temperature T.

Rather than trying to determine simultaneously these two variables, one can replace equation (4) by the follow-

ing one, where the forcing terms depending on R and Q are replaced by a single equivalent one

$$\begin{cases} C\dfrac{dT}{dt} + \displaystyle\sum_{i=1}^{3} h_v S_i (T - \theta_i(0,t)) = Q' \quad [0,\tau] \\ T(0) = 0 \end{cases} \tag{5}$$

The reconstruction algorithm that will be presented in the sequel enables to recover accurately the equivalent load Q'. If the actual thermal load Q is known, by monitoring for example the instant power of internal gains, then it is possible to recover R. Indeed, comparing (5) and (4) yields $Q' + \rho_a c_a R(T - T^a) = Q$ thus

$$R = \frac{Q - Q'}{\rho_a c_a (T - T^a)} \tag{6}$$

We also make here some additional simplifying assumptions. First, we consider that both the ambient and the external temperatures can be measured easily. With T^a and T^s known, the contribution of all terms depending on them can be eliminated from the response using the linearity of the equations. In order to simplify notations, we will thus set $T^a = T^s = 0$ in what follows, without loss of generality. However, if T^a or T^s were not known, it would be possible to add them in the list of the unknowns: the proposed methodology enables one to recover them in the same way in which the sky temperature T^∞ is recovered.

In the same way, in equations (1) to (5), all initial temperatures are set to zero. This choice was made to further simplify the presentation. Note however that the simultaneous reconstruction of forcing terms and initial states is possible with the same experimental setup. We refer to Bourquin and Nassiopoulos (2010) for further details.

With these simplifying assumptions, the problem now consists in searching $\{Q', \Phi, T^\infty\}$ that minimize the data misfit

$$\frac{1}{2} \sum_{\ell=1}^{4} \int_0^\tau \left(\vartheta_\ell - \vartheta_\ell^d \right)^2 dt \tag{7}$$

where $\{\vartheta_\ell\}_{\ell=1}^4 \triangleq \{\theta_1(0), \theta_1(L_1), \theta_2(0), \theta_3(0)\}$ denotes the values at sensor locations of the output of the model (*i.e.* the set of equations (1)-(2)-(3)-(5)) and $\{\vartheta_\ell^d\}_{\ell=1}^4$ denotes the actual measurements provided by the sensors.

This problem is, by nature, ill-posed in the sense of Hadamard (Engl, Hanke, and Neubauer (1994)). As a matter of fact, heat conduction is a diffusive phenomenon with smoothing properties: high variations in the initial state or in boundary conditions tend to disappear with time. As a consequence, any reverse procedure where one tries to recover the unknown causes based on their effects tends to create spurious oscillations. If a solution exists, the numerical procedure is subject to instabilities due to a dramatic amplification of round-off errors. For the solution of such problems a suitable regularization technique is therefore required. In order to deal with ill-posedness of the problem, we use Tikhonov regularization, which consists in adding a regularization term to the data misfit. With the notation

$$\begin{aligned} u &= \{u_1, u_2, u_3\} \\ &= \{Q', \Phi, T^\infty\} \end{aligned}$$

the minimization problem writes

$$\begin{gathered} \text{Find } u \in \mathcal{V} \text{ such that} \\ J(u) = \inf_{\tilde{u} \in \mathcal{V}} J(\tilde{u}) \end{gathered} \tag{8}$$

where

$$J(u) = \frac{1}{2} \sum_{\ell=1}^{4} \int_0^\tau \left(\vartheta_\ell - \vartheta_\ell^d \right)^2 dt + \varepsilon \|u\|_{\mathcal{V}}^2 \tag{9}$$

The second term in J is the so-called Tikhonov regularization term, $\|\cdot\|_{\mathcal{V}}$ denotes the norm in $\mathcal{V}$ and ε stands for the regularization parameter: it is a small real positive constant. The regularization term provides convexity to J so that a unique minimum exists.

The choice of space $\mathcal{V}$, termed the control space, is dependent on the *a priori* assumptions on the unknown u. It was shown in Bourquin and Nassiopoulos (2010) that the choice of a regular space H^1 is more efficient than a L^2 type space, which is the usual choice in literature. The advantage relies on the fact that in L^2, the value at the final time of the time-varying functions cannot be recovered correctly whereas it is the most important output for most applications, such as the one treated here.

We thus seek the unknowns in the Sobolev space

$$\mathcal{V} = \left(H^1(0,\tau) \right)^3$$

endowed with the scalar product $(\cdot,\cdot)_{\mathcal{V}}$ defined by

$$\begin{aligned} (v,w)_{\mathcal{V}} &= \left(\{v_\ell\}_{\ell=1}^4, \{w_\ell\}_{\ell=1}^4 \right)_{\mathcal{V}} \\ &= \sum_{\ell=1}^{4} \int_0^\tau \gamma_\ell^0 v_\ell w_\ell \, dt + \int_0^\tau \gamma_\ell^1 \frac{dv_\ell}{dt} \frac{dw_\ell}{dt} \, dt \\ &\qquad \forall v, w \in \mathcal{V} \end{aligned} \tag{10}$$

In the above, γ_ℓ^0 and γ_ℓ^1, for $\ell = 1..4$, are tuning coefficients that balance the importance of the respective terms.

MINIMIZATION PROCEDURE

Gradient type algorithms can be put to work for the minimization of J. The adjoint method provides an easy-to-implement way to assess the gradient ∇J of J involved in such algorithms (Alifanov (1994), Jarny, Özisik, and Bardon (1991)). Next follows the description of this method applied to the resolution of (8).

By definition, the gradient ∇J of J is given by

$$J(u + \delta u) - J(u) = (\nabla J, \delta u)_{\mathcal{V}} + O\|\delta u\|_{\mathcal{V}}^2 \quad \forall \delta u \in \mathcal{V} \tag{11}$$

We now introduce the adjoint state corresponding to the set of functions $\{p_1, p_2, p_3, q\}$ verifying the set of equations

$$\begin{cases} -\rho_1 c_1 \dfrac{\partial p_1}{\partial t} - \dfrac{\partial}{\partial x} k_1 \dfrac{\partial p_1}{\partial x} = \\ \quad (\theta_1(0,t) - \vartheta_1^d(t))\delta_{1,0} \\ \quad +(\theta_1(L_1,t) - \vartheta_2^d(t))\delta_{1,L_1} & [0,L_1]\times[0,\tau] \\ \\ -k_1 \dfrac{\partial p_1(0,t)}{\partial x} + (2h_r + h_v)p_1(0,t) \\ \quad -h_r(p_2(0,t) + p_3(0,t)) \\ \quad -h_v q = 0 & [0,\tau] \\ \\ k_1 \dfrac{\partial p_1(L_1,t)}{\partial x} + (h_r + h_v)p_1(L_1,t) = 0 & [0,\tau] \\ \\ p_1(x,T) = 0 & [0,L_1] \end{cases} \tag{12}$$

$$\begin{cases} -\rho_2 c_2 \dfrac{\partial p_2}{\partial t} - \dfrac{\partial}{\partial x} k_2 \dfrac{\partial p_2}{\partial x} = \\ \quad (\theta_2(0,t) - \vartheta_3^d(t))\delta_{2,0} & [0,L_2]\times[0,\tau] \\ \\ -k_2 \dfrac{\partial p_2(0,t)}{\partial x} + (2h_r + h_v)p_2(0,t) \\ \quad -h_r(p_1(0,t) + p_3(0,t)) \\ \quad -h_v q = 0 & [0,\tau] \\ \\ k_2 \dfrac{\partial p_2(L_2,t)}{\partial x} + h_s p_2(L_2,t) = 0 & [0,\tau] \\ \\ p_2(x,T) = 0 & [0,L_2] \end{cases} \tag{13}$$

$$\begin{cases} -\rho_3 c_3 \dfrac{\partial p_3}{\partial t} - \dfrac{\partial}{\partial x} k_3 \dfrac{\partial p_3}{\partial x} = \\ \quad (\theta_3(0,t) - \vartheta_4^d(t))\delta_{3,0} & [0,L_3]\times[0,\tau] \\ \\ -k_3 \dfrac{\partial p_3(0,t)}{\partial x} + (2h_r + h_v)p_3(0,t) \\ \quad -h_r(p_1(0,t) + p_2(0,t)) \\ \quad -h_v q = 0 & [0,\tau] \\ \\ k_3 \dfrac{\partial p_3(L_3,t)}{\partial x} + (h_v + h_r)p_3(L_3,t) = 0 & [0,\tau] \\ \\ p_3(x,T) = 0 & [0,L_3] \end{cases} \tag{14}$$

$$\begin{cases} -C\dfrac{dq}{dt} + \displaystyle\sum_{i=1}^{3} h_v S_i(q - p_i(0,t)) = 0 & [0,\tau] \\ q(T) = 0 \end{cases} \tag{15}$$

In the above, $\delta_{i,0}$ (respectively, δ_{i,L_i}) denotes the Dirac function in $[0,L_i]$ equal to 1 at point 0 (respectively, at point L_i), and zero elsewhere. The problems (12) to (15), that constitute the so-called adjoint system of equations, have the same structure as the model equations (1)-(2)-(3)-(5). The difference relies on the right-hand-side terms and on the fact that the time evolution is reversed. With a suitable change of variables in time, they can be solved with the same numerical tools as the model equations. This constitutes the great advantage of the adjoint method.

We set

$$\begin{aligned} X_1 &= q \\ X_2 &= p_1(L_1,t) + (1-\alpha)p_2(0,t) + \int_0^{L_3} \alpha p_3\, dx \\ X_3 &= h_r p_1(L_1,t) + h_r p_3(L_3,t) \end{aligned}$$

At this point, we consider the following problems

$$\begin{gathered} \text{Find } P_j \in H^1(0,\tau) \text{ such that} \\ \int_0^\tau X_j w\, dt = \int_0^\tau P_j w\, dt + \int_0^\tau \frac{dP_j}{dt}\frac{dw}{dt}\, dt \end{gathered} \tag{16}$$

$\forall w \in H^1(0,\tau)$ for $j = 1..3$.

The three last problems are, once again, standard problems that can be solved, for instance, with standard finite element codes.

According to the well-established optimal control theory (Lions (1968)), the gradient of the functional J is given, in a straightforward way, by

$$\nabla J = \{P_j + \varepsilon u_j\}_{j=1}^3 \tag{17}$$

For a detailed proof of this, one can refer to also Bourquin and Nassiopoulos (2010).

Once the gradient computed using the adjoint state, gradient based algorithms can be put to work. In its most basic form, the gradient algorithm consists in incrementing the variables with the descent direction in every iteration n:

$$u_{n+1} = u_n + \rho_n \nabla J(u_n)$$

ρ_n being the optimal step that minimizes the functional J in the descent direction. When the functional is convex, which is the case here, the successive points u_k tend to the minimum of J. Of course, more efficient algorithms, such as the conjugate gradient or other Krylov based algorithms can be put to work. In all cases, determining the gradient entails one computation of the set of equations (1)-(2)-(3)-(5), one computation of the set of equations (12)-(13)-(14)-(15) followed by the computation of the three problems (16). All these problems are standard ones and can be solved with usual tools.

NUMERICAL RESULTS

The results below show numerical evidence of the performance of the approach described so far. The test protocol is the following. First, a direct simulation with known arbitrary sources, obtained using the TRNSYS code (TRNSYS16 (2006)), is conducted. The values of the resulting temperature fields on sensor locations are recorded. These measurements are then used as data for

the reconstruction algorithm, and the results of the reconstruction are compared to the prescribed target functions. The model equations (1) to (3) as well as their corresponding adjoint equations are discretized in space with P1 finite elements. An implicit Euler scheme is used for time integration for all model and adjoint equations. The time interval is split into 100 time-steps.

The conjugate gradient algorithm is put to work here. The iterations are stopped when

$$\sum_{\ell=1}^{4} \int_0^{\tau} \left(\vartheta_\ell - \vartheta_\ell^d\right)^2 dt < 10^{-6}.$$

Figures 2 to 4 compare the reconstructed functions Q', Φ and T^∞ to the actual target ones when convergence is reached. The good overall correspondence of the target and reconstructed functions shows that the algorithm is successful in recovering the unknowns.

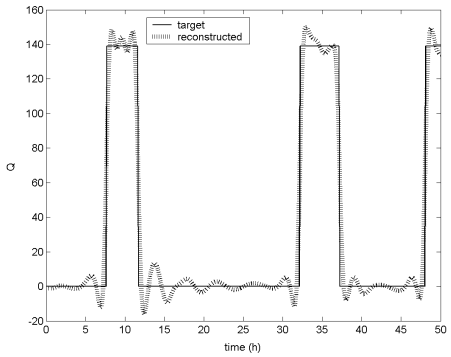

Figure 2: Equivalent zone gains Q': target and reconstructed functions

In particular, figure 2 proves the possibility to reconstruct the equivalent source term within the zone, which results of both the convective heat source Q and the heat transmitted through air ventilation at rate R. If we assume that the convective heat Q is measured by other means, *e.g.* using electrical power sensors in case of an electric device, then the ventilation rate can be recovered using (6). Hence, combining some extra sensors or any other way to estimate internal gains makes it possible to recover ventilation (or infiltration) rates using temperature sensors and the inverse modeling.

In the presented numerical simulations, the observation period lasts 2 days. The inverse computations were carried on with a standard personal computer (Pentium IV processor, with $1.6GHz$ CPU) and lasted less than a minute. Although the computational cost depends on the space discretization and the number of time-steps, their

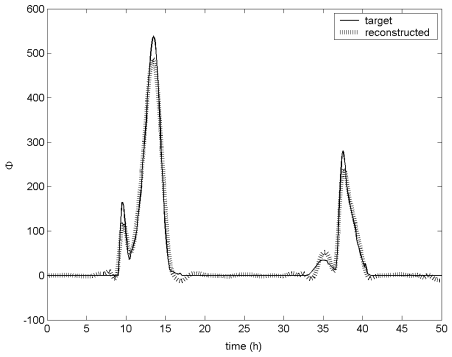

Figure 3: Incident solar radiation Φ: target and reconstructed functions

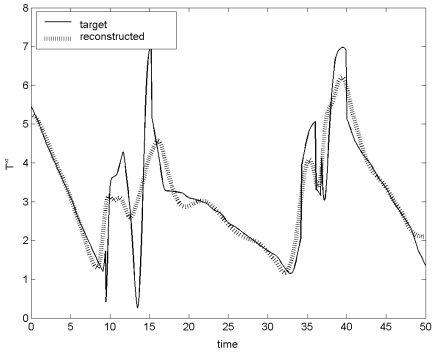

Figure 4: Sky equivalent temperature T^∞: target and reconstructed functions

duration stays far shorter than the typical time constants of building components. Thus, the procedure proves suitable for real-time applications.

CONCLUSION

The work presented here provides a conceptual framework for the development of low-cost and easy-to-implement monitoring systems allowing to distinguish between the occupation and the environmental effects on energy consumptions. The proposed method is based on a inversion procedure combining in an optimal way the detailed model of the building envelope and the measurements obtained from temperature sensors. The inversion procedure aims at reconstructing the unknown source terms such as solar shortwave radiation, longwave radiation or internal gains. Once all the right-hand side terms reconstructed, the model enables to quantify the various convective, radiative and conductive heat transfers between the building and its environment and between the different components of the building envelope.

The benefits of the approach are numerous:

- Only temperature, and, in some cases, power consumption sensors are needed.
- The instrumentation is non intrusive: the number of sensors stays small and only surface sensors are needed.
- The procedure builds upon a detailed model which uses parameters referring to real physical characteristics.
- The algorithms can be implemented very easily with standard computational tools.
- Its speed and accuracy makes the whole procedure suited for real-time applications.

This paper shows some preliminary results of on-going research in this direction. Possible extensions consist in adapting the numerics for the simultaneous identification of both the state and the intrinsic characteristics of the building, such as material thermal properties.

The test-case under study here is an extremely simplified example combining most of the heat transfer phenomena within a building. We claim that the same methodology can be applied successfully to complex buildings provided a suitable multizone model is available. The proposed approach paves the ground for the development of accurate, fast and easy-to-implement monitoring systems.

REFERENCES

Alifanov, O. M. 1994. *Inverse Heat Transfer Problems*. Springer-Verlag, New York.

Bourquin, F., and A. Nassiopoulos. 2010. "Temperature assimilation with accurate final state." *Submitted in Int. J. of Heat and Mass Transfer*.

Branco, G., B. Lachal, P. Gallinelli, and W. Weber. 2004. "Predicted versus obsevred heat consumption of a low energy multifamily complex in Switzerland based on long-term experimental data." *Energy and Buildings* 36:543–555.

Burgess, J., and M. Nye. 2008. "Re-materialising energy use through transparent monitoring systems." *Energy Policy* 36:4454–4459.

Clarke, J. A. 2001. *Energy simulation in building design*. Butterworth Heinemann.

Clarke, J.A., S. Conner, G. Fujii, V. Geros, G. Jóhannesson, C.M. Johnstone, S. Karatasou, J. Kima, M. Santamouris, and P.A. Strachan. 2004. "The role of simulation in support of Internet-based energy services." *Energy and Buildings* 36 (8): 837–846.

Engl, H. W., M. Hanke, and A. Neubauer. 1994. *Regularization of Inverse Problems*. Kluwer Academic Publishers.

Glaser, S. D., and A. Tolman. 2008. "Sense of sensing: from data to informed decisions for the built environment." *Journal of Infrastructure Systems* 14 (1): 5–14.

Haves, P., T. Salsbury, D. Claridge, and M. Liu. 2001, August. "Use of whole building simulation in on-line performance assessment: modeling and implementation issues." *Senventh International IBPSA Conference Building Simulation 2001*.

Jarny, Y., M. N. Özisik, and J. P. Bardon. 1991. "A general optimization method using adjoint equation for solving multidimensional inverse heat conduction." *Int. J. Heat Mass Transfer* 34 (11): 2911–2919.

Krüger, E., and B. Givoni. 2008. "Thermal monitoring and indoor temperature predictions in a passive solar building in an arid environment." *Building and Environment* 43:1972–1804.

Lions, J.-L. 1968. *Optimal control of systems gouverned by PDEs*. Dunod.

Liu, M. 1999. "Improving building energy system performance by continuous commissioning." *Energy Engineering* 96 (5): 46–57.

MacDonald, J. M., and D. M. Wasserman. 1989. "Investigation of metered data analysis methods for commercial and related buildings." *Oak Ridge National Laboratory report*, vol. Rep. CON-279. pdf-imprime.

Madsen, H., and J. Holst. 1995. "Estimation of continuous-time models for the heat dynamics of a

building." *Energy and Buildings* 22:67–79. pdf-imprime.

Neumann, C., and D. Jacob. 2008. "BuildingEQ: Guidelines for the Evaluation of Building Performance." Technical Report, Fraunhofer Institute for Solar Energy Systems.

O'Sullivan, D. T. J., M. M. Keane, D. Kelliher, and R. J. Hitchcock. 2004. "Improving building operation by tracking performance metrics throughout the building lifecycle (BLC)." *Energy and Buildings* 36 (11): 1075–1090.

Piette, M. A., S. K. Kinney, and P Haves. 2001. "Analysis of an information monitoring and diagnostic system to improve building operations." *Energy and Buildings* 33:783–791.

Richalet, V., F. P. Neirac, F. Tellez, and J. J. Bloem. 2001. "HELP (House energy labeling procedure): methodology and present results." *Energy and Buildings* 33:229–233.

Salsbury, T., and R. Diamond. 2005. "Performance validation and energy analysis of HVAC systems using simulation." *Energy and Buildings* 32 (1): 5–17.

Santamouris, M., ed. 2005. *Energy performance of residential buildings: a practical guide for energy rating and efficiency*. Earthscan Publishers.

Subbarao, K., J. D. Burch, C. E. Hancock, A. Lekov, and J. D. Balcomb. 1988. "Short-term energgy monitoring (STEM): application of the PSTAR method to a residence in Fredericksbourg, Virginia." *Solar Energy esearch Institute report*, vol. Rep. TR-254-3356. pdf-imprime.

TRNSYS16. 2006. User manual.

NOMENCLATURE

Q	Real convective zone gains (W)
Q'	Equivalent zone gains (W)
R	Ventilation rate ($m^3.s^{-1}$)
Φ	Incident solar radiation ($W.m^{-2}$)
T	Zone temperature (K)
T^a	External ambient temperature (K)
T^s	Ground temperature (K)
T^∞	Sky equivalent temperature (K)
θ_i	Temperature within wall i (K)
t	Time variable ($t \in [0,\tau]$)
τ	Length of observation period (s)
x	Space variables in domains $[0,L_i]$
L_i	Width of wall i, $i = 1..3$ (m)
u	The set of unknown functions: $u = \{u_i\}_{i=1}^n = \{Q', \Phi, T^\infty\}$
$\{\vartheta_i^d\}_{i=1}^m$	Measurements delivered by sensors
$\{\vartheta_i\}_{i=1}^m$	Model response at sensor locations: $\{\vartheta_i\}_{i=1}^4 \triangleq \{\theta_1(0), \theta_1(L_1), \theta_2(0), \theta_3(0)\}$
J	Tikhonov regularized functional
∇J	The gradient of J
p_i	Adjoint functions corresponding to θ_i
q	Adjoint function corresponding to T
X_i	Components of the gradient of J in L^2
P_i	Components of the gradient of J in H^1
k_i	Conductivity of wall i ($W.m^{-1}.K^{-1}$)
ρ_i	Mass density of wall i ($kg.m^{-3}$)
c_i	Specific heat capacity of wall i ($J.kg^{-1}.K^{-1}$)
ρ_a	Mass density of air ($kg.m^{-3}$)
c_a	Specific heat capacity of air ($J.kg^{-1}.K^{-1}$)
C	Heat capacity of zone ($J.K^{-1}$)
h_v	Convective coefficient ($W.m^{-2}.K^{-1}$)
h_r	Radiative coefficient ($W.m^{-2}.K^{-1}$)
h_r	Conductive coefficient ($W.m^{-2}.K^{-1}$)
S_i	Surface of wall i (m^2)